ChemComm

Accepted Manuscript

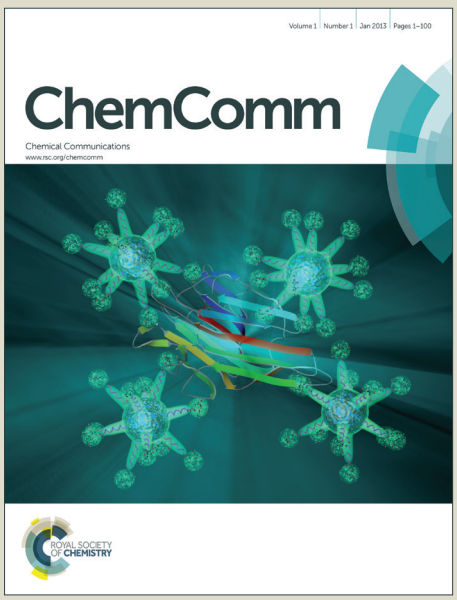

ROYAL SOCIETY OF CHEMISTRY

www.rsc.org/chemcomm

Journal Name

RSCPublishing

COMMUNICATION

Sulfur gradient-distributed CNF composite: a self-inhibiting cathode for binder-free lithium-sulfur batteries

Cite this: DOI: 10.1039/x0xx00000x

Received ooth January 2012,
Accepted ooth January 2012

DOI: 10.1039/x0xx00000x

www.rsc.org/

Kun Fu,[a,†] Yanpeng Li,[b,c,†] Mahmut Dirican,[a] Chen Chen,[a] Yao Lu,[a] Jiadeng Zhu,[a] Yao Li,[c] Linyou Cao,[b] Philip D. Bradford[a] and Xiangwu Zhang[a,*]

A self-inhibiting, gradient sulfur structure was designed and developed by the synthesis of carbon nanofiber-sulphur composite via sulfur vapor deposition method for use as a binder-free sulfur cathode, exhibiting high sulfur loading (2.6 mg cm^{-2}) and high sulfur content (65%) with a stable capacity of > 700 mAh g^{-1}.

Lithium-sulfur batteries are promising electrochemical power sources for various applications, including plugin electric vehicles (PEVs), due to their high energy density, large capacity, safe operating voltage, and potential for low cost production. [1–3] Sulfur has a theoretical capacity of 1675 mAh g^{-1}, which is one order of magnitude greater than that of conventional cathode materials used in lithium-ion batteries. However, the study of lithium-sulfur batteries faces several challenges, including low sulfur utilization, low coulombic efficiency and rapid capacity loss during repeated cycling. These problems are caused by the low electronic conductivity of sulfur and its discharge products, and the diffusion, shuttling effect, and side reactions of soluble polysulfides produced during electrode reactions.[4] Figure 1a shows the diffusion and shuttling of polysulfides in the electrolyte between a conventional sulfur cathode and a lithium metal anode, and also the resultant deposition of insoluble Li_2S on the anode due to side reactions between dissolved polysulfides with lithium.

The most commonly studied approach to solve these problems is to make sulfur-carbon composites. Many sulfur-carbon composites not only have increased electrical conductivity, but also store the active material inside the carbon matrix. However, most sulfur-carbon composites have low tap densities and their synthesis methods, including carbon preparation and sulfur impregnation, are typically complicated and high cost, which limit their possible use in lithium-sulfur batteries.[5–14] Recently, both A. Manthiram's and S.S. Zhang's groups have independently introduced the dual-layer sulfur cathode concept that a porous carbon layer was placed between a conventional sulfur cathode and a separator to capture the migrating polysulfides from the cathode during electrochemical reactions, and a significant improvement was achieved in the sulfur utilization and capacity retention.[15,16] Figure 1b shows the schematic configuration of a lithium-sulfur cell with the dual-layer sulfur cathode. The carbon interlayer can not only reduce the interfacial resistance in the cathode but also prevent polysulfides from migrating to the anode.[16] However, one challenge of this dual-layer configuration is the relative lower sulfur content if the weight of the entire electrode including the carbon interlayer is taken into consideration. The carbon interlayer decreases the specific capacity of cathode and reduces the overall energy density of a lithium-sulfur cell, which makes the goal of replacing lithium-ion batteries more challenging. Therefore, it is important to obtain a cathode that can simultaneously have high sulfur loading/content and good electrochemical performance.

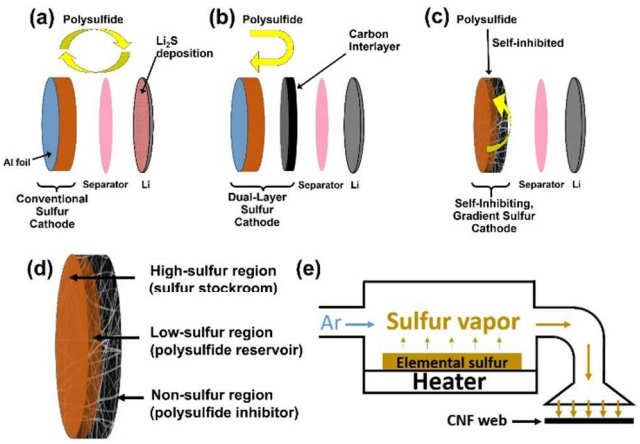

Fig.1 Schematic configuration of a lithium-sulfur cell with a conventional sulfur cathode (a), a dual-layer sulfur cathode (b), and a self-inhibiting, gradient sulfur cathode (c), respectively. (d) Schematic of the self-inhibiting, gradient sulfur cathode with high-sulfur region, low-sulfur-region, and non-sulfur region. (e) Schematic of the synthesis process of the carbon nanofiber-sulfur (CNF-S) composite.

To address this challenge, a new lithium-sulfur configuration using a self-inhibiting, gradient sulfur composite cathode is presented in this communication and is shown schematically in Figure 1c. The sulfur composite has a gradient sulfur distribution along the composite's thickness which forms a high-sulfur, a low-sulfur, and a non-sulfur

region (Figure 1d). The high-sulfur region is a sulfur resource that functions as sulfur electrode while the nano-carbon supporting network decreases the internal charge transfer resistance. The low-sulfur region operates as a reservoir to localize the dissolved polysulfide and the non-sulfur region acts as an inhibitor to prevent polysulfide migration between electrodes. In the battery, the three regions work synergistically to provide high conductivity and inhibit the polysulfides from leaving the cathode structure to achieve high sulfur utilization and good cycling stability. As a result, this new self-inhibiting, gradient sulfur cathode structure can address the challenges faced by conventional sulfur cathodes and outperform dual-layer cathodes when the mass of the carbon component is taken into account in the specific capacity.

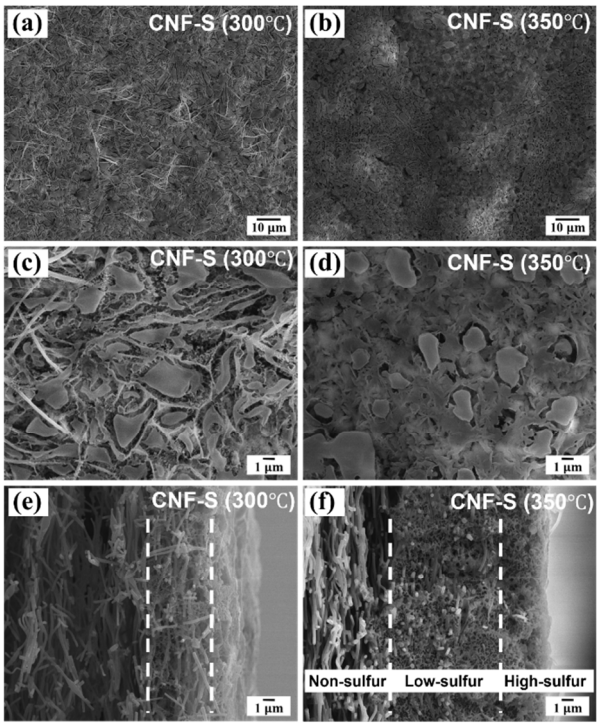

Fig. 2 SEM images of the top view of CNF-S (300 °C) (a,c) and CNF-S (350 °C) (b,d). SEM images of the side view of CNF-S (300 °C) (e) and the CNF-S (350 °C) (f).

The schematic synthesis of the CNF-S composite is shown in Figure 1e. This sulfur vapor deposition provides a simple, continuous, and economical strategy to produce cathodes at high speed and low cost. The method of sublimation following condensation shows a promising industrial potential and has been used by M. Hagen et al. in preparing CNT-S cathodes.[17] In this work, the furnace temperature was controlled at 250, 300, and 350 °C to produce sulfur vapor and obtain CNF-S composites with sulfur loading of 0.5, 1.7, and 2.6 mg cm^{-2}, respectively. The CNF web had a density of 1.4-1.5 mg cm^{-2} with a thickness of around 0.15 mm. The top view of the CNF-S composites prepared at furnace temperatures of 300 and 350 °C shows a dense sulfur coating on the CNF cloth surfaces, as shown in Figure 2a and 2b. The CNF-S prepared at furnace temperature of 250 °C exhibited a totally different surface morphology that consisted of a light sulfur coating on the individual CNFs instead of covering the whole cloth's surface (Figure S1). At the higher furnace temperatures, dense sulfur coating was formed on the surface, demonstrating the morphology we proposed in Figure 1d. In the CNF-S (300 °C) composite, a high-sulfur region was formed with a rough plateau topology where regions of thicker sulfur deposition make up the sulfur plateaus and some of uncoated individual CNFs were only lightly coated on the surface (Figure 2c). In the CNF-S (350 °C) composite, the entire CNF cloth was covered by sulfur and the sulfur coating appears denser than that in the CNF-S (300 °C) composite (Figure 2d). The gradient sulfur distribution can be observed clearly from the cross-sectional SEM images as shown in Figure 2e and 2f.

To confirm the gradient CNF-S structure, Raman spectroscopy was applied and sulfur peaks were detected on one side of CNF-S composite and the other side cannot be detected as shown in Figure 3a, confirming the gradient sulfur distribution along the cross-section of the CNF web. X-ray diffraction (XRD) patterns are shown in Figure 3b, indicating that a large amount of sulfur remained on the composite surface instead of being embedded inside the carbon material.

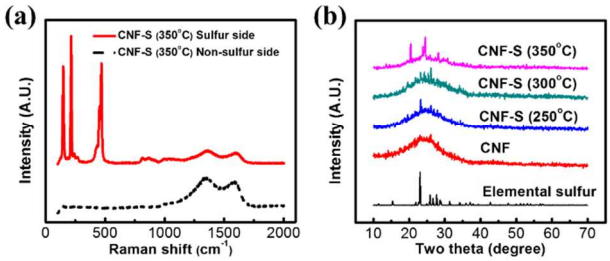

Fig.3 Raman spectra of top and bottom sides of CNF-S (350oC) composite (a). XRD spectra of elemental sulfur, CNF web, and CNF-S composites (b).

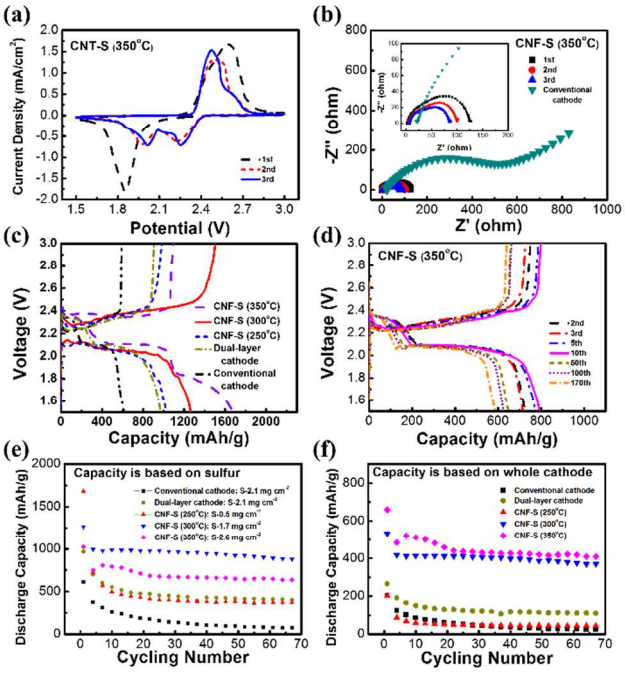

Fig.4 (a) Cyclic voltammetry profiles of CNF-S (350 °C). (b) Electrochemical impedance spectroscopy plot of CNF-S (350 °C) compared with conventional sulfur electrode. (c) Initial discharge-charge curves of conventional sulfur electrode, CNF-inserted dual-layer sulfur electrode, and CNF-S composites at 100 mA g^{-1}. (d) Discharge-charge curves of CNF-S (350 °C) at 100 mA g^{-1}. (e,f) Cycling performance of different cathode configurations based on sulfur and overall electrode, respectively.

Cyclic voltammetry (CV) plots of the CNF-S (350 °C) composite, in the first three cycles, are shown in Figure 4a. The CNF-S (350 °C) composite exhibited one broad reduction peak with a large current density at 1.85 V in the first cycle because of the poor conductivity caused by the high sulfur loading. After the first cycle, reduction peaks turned to normal, indicating the good and stable sulfur reduction process in the CNF structure. Impedance analysis indicates this novel CNF-S composite (350 °C) has higher conductivity than the conventional sulfur cathode (Figure 4b).

The initial discharge-charge curves of the conventional sulfur cathode and the CNF-S cathodes prepared at different temperatures are shown in Figure 4c. The third plateau of CNF-S (350 °C) below 1.8 V was likely due to the irreversible reduction of $LiNO_3$, but no evident $LiNO_3$ reduction plateau was observed on other samples. The initial (Figure 4c) and subsequent discharge-charge (Figure 4d) curves correlated well with the CV curves (Figure 4a) for the CNF-S (350 °C) composite. A sloping voltage plateau starting at 2.1 V with a significant voltage hysteresis and a much larger discharge capacity for the initial discharge of CNF-S (350 °C) is apparent in Figure 4c. In the following 10 cycles, as shown in Figure 4d, the prolonged low-voltage plateau and decreased voltage difference between discharge and charge curves showed that more sulfur was activated and participated in the reduction reaction, indicating that sulfur was rearranged to favourable electrochemical positions in the CNF web.[16]

In Figure 4e, CNF-S (250 °C), CNF-S (300 °C), and CNF-S (350 °C) composites exhibited different cycling behaviours. Based on solely the mass of sulfur, CNF-S (250 °C) cathode delivered the highest discharge capacity (>1600 mAh g^{-1}) in the first cycle, but encountered a rapid capacity loss during the subsequent cycles. The initial high discharge capacity approaching the theoretical capacity of sulfur (1675 mAh g^{-1}) is reasonable because of the high carbon content (~80%) and the nanosized sulfur particles formed during the sulfur vapor deposition. The rapid capacity loss was probably due to the light sulfur deposition in the CNF-S (250 °C) structure (Figure S1), which made it more difficult to form a saturated polysulfide/electrolyte condition. However, more work is needed to completely understand the mechanism of capacity loss. From Figure 4e, it is seen that CNF-S (300 °C) and CNF-S (350 °C) composites have more stable cycling behaviour. The CNF-S (300 °C) composite maintained a high capacity value of around 1000 mAh g^{-1} with a large capacity retention of around 95% at the 50th cycle. The CNF-S (350 °C) composite showed slight capacity decrease in the first 20 cycles, but remained at a stable capacity of 700 mAh g^{-1} in the subsequent cycles. These results indicate that among all samples studied, the CNF-S (300 °C) composite had the highest specific capacity after prolonger cycling. SEM observations show that the sulfur gradient structure was still maintained after cycling, as shown in Figure S2.

So far, most researchers have focused on improving the capacity and cycling life of sulfur cathodes.[18,19] The capacity values in most literature reports have been calculated based solely on the mass of sulfur. However, if a sulfur cathode has low sulfur loading or sulfur content, the high capacity calculated based on sulfur may not reflect the true electrochemical performance of the cathode due to the presence of a large amount of inactive materials such as polymer binder, carbon black, and Al foil. Our CNF-S composites have high sulfur loading and high sulfur content, and they can be potentially used as sulfur cathodes without the presence of polymer binder, carbon black, and Al foil. Hence, the high capacities and good cycling performance of the CNF-S composites will directly result in good electrochemical performance of the batteries. Figure 4f compared the capacities and cycling performance of CNF-S composites with those of conventional and dual-layer sulfur cathodes by normalizing the capacities based on the total mass of the electrode configuration including the carbon interlayer. It is seen that CNF-S (300 °C) and CNF-S (350 °C) composites always exhibited significantly higher capacities than other cathodes during cycling. The capacity of 400 mAh g^{-1} is considered to be the lithium-ion cell equivalent as typical cathodes in lithium-ion batteries deliver around 200 mAh g^{-1} capacity but with higher operating voltage (~4 V) than lithium-sulfur batteries.[19] Note that since the CNF-S (350 °C) composite had high sulfur loading (2.6 mg cm^{-2}) and high sulfur content (~65%), the cycling results are very promising and this novel CNF-S electrode design shows great potential as one high-capacity cathode candidate for increasing the total energy density of lithium-sulfur cells. For larger-format batteries (e.g., 18650 cells or pouch cells), we believe that due to the presence of the free-standing, conductive CNF web, it is possible to avoid the use of polymer binder and Al foil, and the feasibility of assembling such binder-free and current collector-free batteries will be demonstrated in future work.

Conclusions

In summary, we have developed a multifunctional CNF-S composite with high sulfur loading (~2.6 mg cm^{-2}) and high sulfur content (~65%) as a promising binder-free cathode for high-energy lithium-sulfur batteries. This CNF-S composite has a unique structure with a gradient sulfur distribution that consists of a high-sulfur region, low-sulfur region, and non-sulfur region through the thickness of CNF web. The CNF-S composite not only has high sulfur loading but also helps to localize the dissolved sulfur and polysulfide. In addition, a novel sulfur vapor deposition strategy was demonstrated and proved to be an effective way to synthesize the carbon-sulfur cathodes, which greatly shortens the composite preparation time, especially the sulfur loading time, from tens of hours to a few minutes. This advanced CNF-S electrode structure with high capacity and good stability provides a promising sulfur cathode with high sulfur content and sulfur loading to compete with conventional S@C composite and cell configuration for lithium-sulfur batteries.

This work was supported by National Science Foundation (CMMI-1231287), Advanced Transportation Energy Center, and ERC Program of the National Science Foundation under Award Number EEC-08212121.

Notes and references

[a] *Department of Textile Engineering, Chemistry and Science, North Carolina State University, Raleigh, NC 27695, USA E-mail: xiangwu_zhang@ncsu.edu*

[b] *Department of Materials Science and Engineering, North Carolina State University, Raleigh, NC 27695, USA*

[c] *Center for Composite Material, Harbin Institute of Technology, Harbin, China*

† The authors contributed equally to this work.

Electronic Supplementary Information (ESI) available: Experimental Information See DOI: 10.1039/c000000x/

1. M. Armand and J.-M. Tarascon, *Nature*, 2008, **451**, 652–657.

2. N.-S. Choi, Z. Chen, S. a Freunberger, X. Ji, Y.-K. Sun, K. Amine, G. Yushin, L. F. Nazar, J. Cho, and P. G. Bruce, *Angew. Chemie*, 2012, **51**, 9994–10024.

3. D. Bresser, S. Passerini, and B. Scrosati, *Chem. Commun.*, 2013, **49**, 10545–10562.

4. Y.-X. Yin, S. Xin, Y.-G. Guo, and L.-J. Wan, *Angew. Chem. Int. Ed. Engl.*, 2013, **52**, 13186–13200.

5. X. Ji, K. T. Lee, and L. F. Nazar, *Nat. Mater.*, 2009, **8**, 500–506.

6. B. Zhang, X. Qin, G. R. Li, and X. P. Gao, *Energy Environ. Sci.*, 2010, **3**, 1531–1537.

7. J. Guo, Y. Xu, and C. Wang, *Nano Lett.*, 2011, **11**, 4288–4294.

8. L. Ji, M. Rao, H. Zheng, L. Zhang, Y. Li, W. Duan, J. Guo, E. J. Cairns, and Y. Zhang, *J. Am. Chem. Soc.*, 2011, **133**, 18522–18525.

9. H. Wang, Y. Yang, Y. Liang, J. T. Robinson, Y. Li, A. Jackson, Y. Cui, and H. Dai, *Nano Lett.*, 2011, **11**, 2644–2647.

10. G. Zheng, Q. Zhang, J. Cha, Y. Yang, and W. Li, *Nano Lett.*, 2013, **13**, 8–13.

11. S. Lu, Y. Cheng, X. Wu, and J. Liu, *Nano Lett.*, 2013, **13**, 2485–2489.

12. W. Zhou, H. Chen, Y. Yu, D. Wang, Z. Cui, F. J. Disalvo, and H. D. Abruña, *ACS Nano*, 2013, **7**, 8801–8808.

13. J. T. Lee, Y. Zhao, S. Thieme, H. Kim, M. Oschatz, L. Borchardt, A. Magasinski, W.-I. Cho, S. Kaskel, and G. Yushin, *Adv. Mater.*, 2013, **25**, 4573–4579.

14. L. Ji, M. Rao, S. Aloni, L. Wang, E. J. Cairns, and Y. Zhang, *Energy Environ. Sci.*, 2011, **4**, 5053.

15. S. S. Zhang, *Electrochem. commun.*, 2013, **31**, 10–12.

16. Y.-S. Su and A. Manthiram, *Nat. Commun.*, 2012, **3**, 1166.

17. M. Hagen, S. Dörfler, H. Althues, J. Tübke, M. J. Hoffmann, S. Kaskel, and K. Pinkwart, *J. Power Sources*, 2012, **213**, 239–248.

18. S. Zhang, *Energies*, 2012, **5**, 5190–5197.

19. M.-K. Song, Y. Zhang, and E. J. Cairns, *Nano Lett.*, 2013, **13**, 5891–5899.

